J. Phys. B: At. Mol. Phys. **20** (1987) 5903-5915. Printed in the UK

Multiple ionisation of Ar atoms by single-electron impact at energies near threshold

H R Kosłowski, J Binder, B A Huber and K Wiesemann

Institut für Exp. Physik, AG II, Ruhr-Universität Bochum, West Germany

Received 1 December 1986, in final form 20 February 1987

Abstract. Multiple ionisation of Ar atoms by single-electron impact is investigated in the energy range from threshold up to about 600 eV. Partial cross sections for the production of Ar^{q+} with $3 \leq q \leq 6$ are measured. In the near-threshold region the ionisation curves can be fitted according to power laws $\sigma \propto (E_{el} - E_{thr})^{\kappa}$, where the exponent κ is found to be smaller than q for high charge states. At higher electron energies the ionisation cross sections show a significant influence of inner-shell ionisation, which becomes the dominant mechanism for the production of high charge states.

1. Introduction

The determination of partial ionisation cross sections, i.e. cross sections for the production of ions in specific charge states q, has a wide range of applications, namely in plasma physics, astrophysics and chemistry. Furthermore, there is also fundamental interest in the process itself, because this leads to a better understanding of the ionisation mechanism.

Many groups have worked on this topic and at present there are many data available. A summary of the research has been given by Tawara *et al* (1985) and a review of the work has been undertaken by Märk and Dunn (1985). Whereas total and partial ionisation cross sections for low charge states are well known, there is still some need for measurements of partial cross sections for the production of highly charged ions. These investigations are quite difficult, in particular at electron impact energies close to the threshold. The threshold region has its importance in different topics: near-threshold cross sections yield information on possible electron correlation effects and they are important for the establishment of charge-state distributions in plasmas with moderate electron temperatures.

The threshold behaviour of the ionisation function was first calculated by Wannier (1953) for single ionisation as well as for multiple ionisation (Wannier 1955). The ionisation function near threshold is expected to be a power law of the form

$$\sigma \sim (E_{el} - E_{thr})^{\kappa(q)}$$

where $(E_{el} - E_{thr})$ is the excess electron energy above threshold and the exponent κ depends on the charge state q of the produced ion.

This dependence has been studied and reviewed in various recent publications (Rau 1984a, b, Read 1985, Grujić 1986) showing the exponent κ to be equal to q, if long-range correlations in the multiple ionisation process are neglected.

This result is obtained by considering the energy phase space of dimension $q+1$, where each dimension corresponds to the final energy E_i of one of the escaping $q+1$

0022-3700/87/215903+13$02.50

electrons. According to energy conservation the excess energy $(E_{el} - E_{thr})$ has to be equal to the sum of all the final electron energies E_i, provided additional excitation of the created ion is neglected. By this condition a hyper-surface is defined in the energetically accessible phase space region $((E_{el} - E_{thr}) \geq E_i \geq 0)$. The area of this surface scales with the excess energy according to $(E_{el} - E_{thr})^q$ and so does the ionisation cross section, which is proportional to this area.

If long-range electron correlation is taken into account calculations predict a slightly larger value of the exponent (Klar and Schlecht 1978, Grujic 1983).

In the case of single ionisation this threshold law has been studied by many authors yielding good agreement with the Wannier law ($\kappa = 1.127$). Multiple-ionisation processes have been studied less frequently (Märk and Dunn 1985). In some cases (e.g. see Kiefer and Dunn 1966 and references therein)—especially for higher charge states—the experiments have been performed at electron energies well above the threshold energy (several eV) due to the limited sensitivity. In this energy range ions may be produced in different electronically excited states with different threshold energies. This complicates the analysis since the ionisation cross section must be considered as a superposition of different state-selective cross sections. It is expected that only these state-selective cross sections obey a simple power law.

Therefore in order to obtain a more detailed test of the theoretical predictions we have measured, besides partial cross sections, state-selective partial cross sections for the production of Ar^{q+} ions ($q = 2, 3$) in long-lived electronically excited states by single-electron impact on Ar atoms.

Furthermore, we have measured partial ionisation cross sections from threshold to an electron energy of about 600 eV. It turns out that these cross sections are influenced by inner-shell ionisation followed by Auger cascades. Above threshold for 2p hole production, inner-shell ionisation is found to be the dominant process for producing highly charged argon ions ($q \geq 4$).

In the following we start with a description of the experimental set-up and the normalisation method used for obtaining absolute partial ionisation cross sections. The cross sections for two- to six-fold ionisation of Ar are presented and contributions of inner-shell ionisation are analysed. Furthermore, partial and state-selective cross sections in a range of a few eV above threshold will be discussed.

2. Experiment

The ions were produced in a small electron impact ion source, extracted by a weak electrostatic field and separated according to their mass/charge ratio by a magnetic sector field. After passing through a collision chamber which can be filled with a target gas the ions were analysed with respect to their kinetic energy in a double hemispherical analyser and finally detected with the aid of a channeltron. A more detailed description of the spectrometer and the ion source can be found elsewhere (Kahlert *et al* 1983, 1985). Because of the unknown detection and extraction efficiency for the ions produced in the ion source the data have to be corrected and normalised to absolute values obtained by other authors. The exact calibration and normalisation procedure was given by Wiesemann *et al* (1986).

The collision chamber and the kinetic energy analyser were only used for the measurement of state-selective cross sections distinguishing ground-state and metastable ions by different kinetic energy gains in an electron capture reaction in a suitable

target gas. In other cases the energy analyser is not necessary but can be used to reduce the beam intensity (a higher resolution leads to smaller transmission) to ensure counting rates less than approximately 1 kHz, guaranteeing a linear response of the channeltron and the attached pulse-shaping amplifiers.

The ion source and wiring were slightly modified compared with previously reported experimental set-ups and figure 1 gives a view of the present situation. The ionisation volume is shielded by a stainless steel grid with respect to a potential of 50 V at the electron collector EC which is used in order to suppress secondary electrons. The electron lens is fed by a voltage of about 80% of the voltage between anode and cathode. This is done by a voltage-dividing network decoupled by an operational amplifier in order to obtain a low output impedance. The cathode potential is controlled using an external programmable power supply and a 10 bit DAC designed to operate with an Apple personal computer. The data aquisition is made with a scan routine while counting the channeltron pulses.

The evaluation of the threshold ionisation function was made with the aid of a LSI 11/23 computer with a mathematical standard procedure using a chi-square test function with statistical weights fitting an analytical function to the measured data. As a sensitive test for the quality of the fit the obtained threshold energy was taken. Only those fits were accepted which yielded energies close to those reported in the literature (e.g. Bashkin and Stoner 1978). Some allowance for contact potentials between anode and cathode of the ion source was made. In all fits this correction

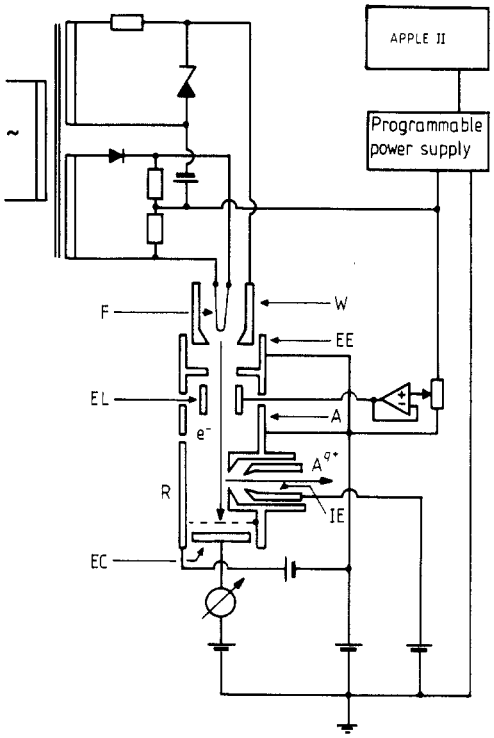

Figure 1. Schematic diagram of the ion source and wiring. F: filament, thoriated tungsten hair pin cathode; W: Wehnelt; EE: electron extraction electrode; EL: electron lens; A: anode; R: repeller electrode; IE: ion extraction; EC: electron collector.

turned out to have the same size of about 1–1.5 eV, which is in agreement with the values expected for the thoriated tungsten (cathode) and stainless steel (anode) combination.

3. Results and discussion

3.1. Partial ionisation cross sections

The measured ionisation curves for the production of multiply charged Ar ions in various charge states are shown in figure 2, the corresponding values are given in table 1. At the marked data points our ionisation functions were fitted to absolute cross sections from Gaudin and Hageman (1967) for $q = 4$ and Schram *et al* (1966) for $q = 3$, 5, 6. The shape of our ionisation function for Ar^{3+} agrees very well with the measurements of other authors, see for example, Tawara *et al* (1985). For charge states $q = 4$, 5, 6 and electron energies below 200, 400 and 600 eV, respectively, no measurements have been reported until now. In regions, where our measurements overlap with respect to electron energy with results of other groups, the agreement is again quite satisfying.

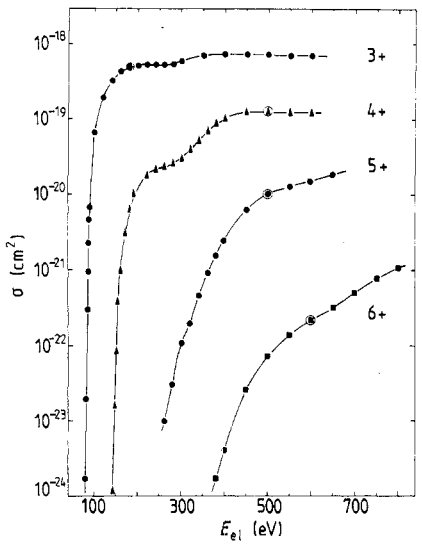

Figure 2. Partial cross sections for electron impact ionisation of Ar. The curves are normalised to absolute values at the marked data points. For reference we have used data from Schram *et al* (1966) (Ar^{3+}, Ar^{5+}, Ar^{6+}) and Gaudin and Hageman (1967) (Ar^{4+}).

The ionisation functions show a shoulder at an electron impact energy of about 250–300 eV. This increase in the cross sections can be attributed to inner-shell ionisation of the ($n = 2$) levels, the binding energies of which are (from Sevier 1979) 245, 247 (2p electron) and 326 eV (2s electron). Singly charged ions produced by this process are characterised by an inner-shell hole and therefore decay via Auger transitions forming multiply charged ions in different charge states (Carlson *et al* 1966). A second process connected with the inner-shell vacancy production is the shake-off mechanism,

Table 1. Partial cross sections for the production of Ar^{q+} $(3 \leq q \leq 6)$ by single-electron impact.

E_{el} (eV)	$\sigma(Ar^{3+})$ $(10^{-19}\ cm^2)$	$\sigma(Ar^{4+})$ $(10^{-20}\ cm^2)$	$\sigma(Ar^{5+})$ $(10^{-21}\ cm^2)$	$\sigma(Ar^{6+})$ $(10^{-22}\ cm^2)$
84.5	0.000 02			
85	0.000 2			
86	0.002			
87	0.008			
88	0.02			
90	0.07			
100	0.62			
120	2.0			
140	3.3			
145		0.000 1		
147		0.002		
150		0.009		
155		0.04		
160	4.2	0.1		
170		0.3		
180	5.0	0.6		
190		1.0		
200	5.1	1.3		
220	5.3	1.8		
240	5.4	2.2		
260	5.3	2.3	0.01	
280	5.5	2.6	0.03	
300	6.0	3.1	0.11	
320		4.0	0.19	
340	7.1	5.2	0.46	
		7.1	0.93	
380		9.0	1.6	0.02
400	7.4	11	2.6	0.04
450	7.5	13	6.5	0.26
500	7.3	13	11	0.72
550	7.2	13	14	1.4
600	7.1	13	16	2.2
650			19	3.3
700				5.0
750				8.0
800				11

where additional electrons are ejected due to the rapid change in the effective core potential.

The influence of inner-shell ionisation is shown in more detail in figure 3, where the cross section for Ar^{3+} ions is fitted by a Lotz formula (Lotz 1967) with suitably chosen parameters. The full curve is a fit to the data points below an electron energy of 250 eV. At higher energies the measured ionisation curve shows a deviation from the fitted curve towards higher cross sections which result from inner-shell ionisation. The difference between the first Lotz formula fit and the measurement (crosses) can be fitted again by a second Lotz formula (broken curve). The sum of both fitted curves gives a very good representation of the experimental results. This example shows the important role of inner-shell vacancies for the production of multiply charged ions

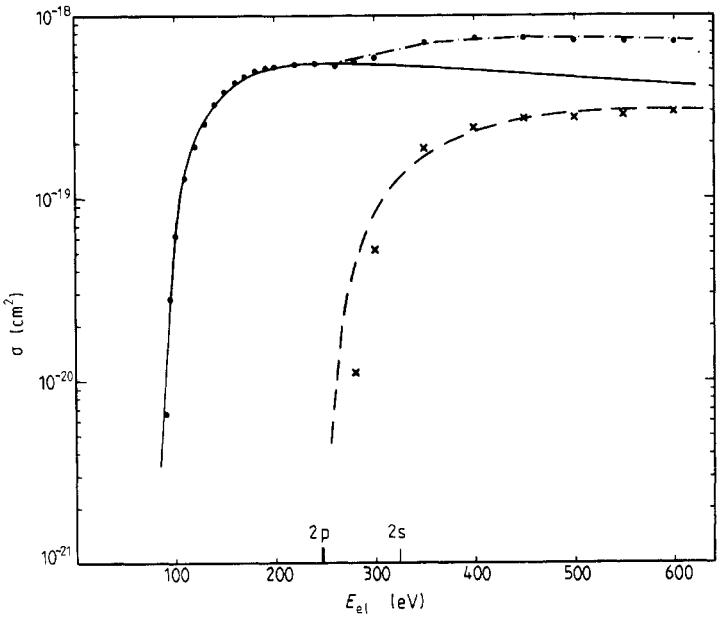

Figure 3. Lotz formula fit of the Ar^{3+} cross section (obtained from the reaction $e^- + Ar \rightarrow Ar^{3+} + 4e^-$). ●, measurement; ——, Lotz formula fit for direct ionisation of the M shell; ×, difference between the measurement and the first fit; - - -, Lotz formula fit for ionisation of the L shell; — · —, sum of both fitted curves.

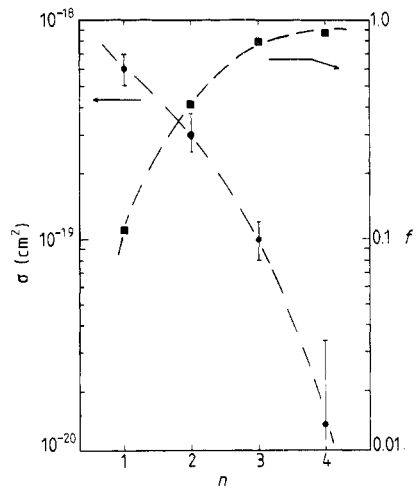

Figure 4. Absolute (σ) and relative (f) cross sections for the production of Ar^{2+}-Ar^{5+} ions via inner-shell vacancies at an electron energy of 600 eV plotted against the number of additionally ejected electrons n where $q = n + 1$.

and therefore explains the complex structure of the ionisation functions. From the partial ionisation cross sections one can estimate the inner-shell contributions for each charge state. In figure 4 the corresponding cross sections are plotted against the number of electrons additionally emitted via Auger cascades and shake-off processes after the production of an L vacancy by 600 eV electrons. Although the absolute cross section decreases with the number of ejected electrons n, the relative contribution of inner-shell processes to the partial ionisation cross section increases with n and becomes about 90% for Ar^{5+}.

The same behaviour was found in multiple ionisation processes occurring in electron–ion collisions (Müller and Frodl 1980). In accordance with our results the relative contributions from L-shell ionisation of Ar^+ ions was found to increase with the final charge state.

3.2. Threshold behaviour of partial and state-selective ionisation cross sections

With decreasing electron impact energies near threshold the ionisation cross section vanishes with zero slope at threshold. From the statistical arguments described in § 1, the cross section should be represented by a scaling power law. In order to prove this, we have measured near-threshold cross sections and fitted the data to a power function. A fit to the Ar^{2+} partial cross section yields an exponent κ of about 2.6, which is greater than expected. Neglecting long-range interactions and taking into account only the phase space density for the outgoing electrons, this exponent should be equal to 2. In fact Brion and Thomas (1968) found such a behaviour for the process $e^- + {}^3He \rightarrow 3e^- + {}^3He^{2+}$ for electron energies up to 25 eV above threshold. In the case of argon the situation is more complicated due to different electronic states of the Ar^{2+} ion with low excitation energies. For the electron excess energies used in our experiment not only Ar^{2+} ions in the ground state are formed but the first two metastable states with excitation energies of 1.7 and 4.2 eV will be populated too. To analyse the production of ions in these different states, the initially formed Ar^{2+} ions were passed through a gas target in the collision chamber and the energy spectra of Ar^+ ions produced in a single-electron-capture reaction were measured with target gases He, Ne and Kr. From the well known reaction schemes (Huber and Kahlert 1983) the internal states of primary ions leading to different peaks in these spectra could be identified. By choosing an appropriate target gas and setting the electrostatic analyser on a certain peak, secondary ions belonging to a known electronic state of the primary Ar^{2+} ions can be detected as a function of the electron impact energy in the ion source, giving a signal proportional to the state-selective ionisation cross section. The results are shown in figure 5 where state-selective cross sections for the production of Ar^{2+} ions in the ground state ^3P and the first metastable states ^1D and ^1S are plotted against the electron impact energy. The values are also summarised in table 2. For an absolute calibration of the data we used the apparent cross section at 50 eV recently reported by Wiesemann *et al* (1987). The fit of the state-selective cross sections to power laws results in exponents of 2.0, 2.3 and 2.0 for the states ^3P, ^1D and ^1S respectively, with an accuracy of 20–30%. The broken curve in figure 5 is the sum of all three curves and it is easy to see that the fit of the partial cross section to a power law will result in a slightly greater exponent since it can be described as a superposition of different shifted power laws.

The same analysis can be made for Ar^{3+} ions. Figure 6 shows the partial cross section which can be fitted to a power law with an exponent of three. However, the

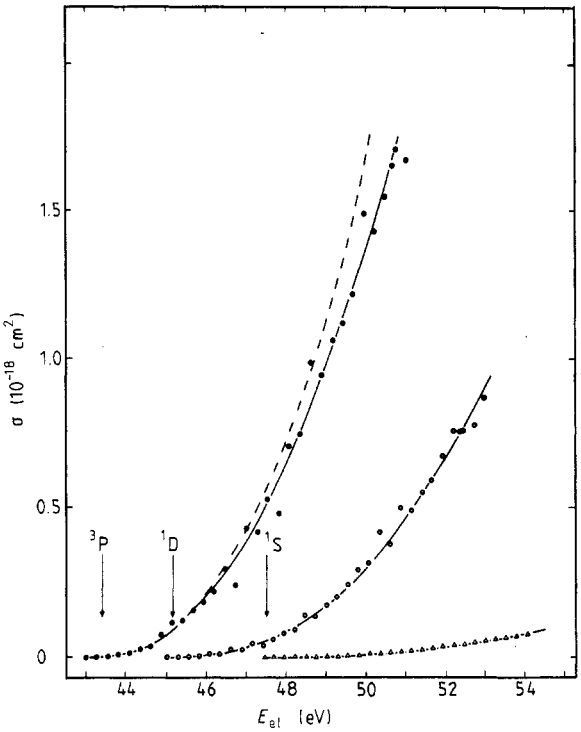

Figure 5. State-selective cross sections for the production of the ^3P ground state (●) and the ^1D (○) and ^1S (△) metastable states of Ar^{2+} (obtained from the reaction $e^- + Ar \rightarrow 3e^- + Ar^{2+}$ (^3P, ^1D, ^1S)). Full curves are fitted power functions and the broken curve is the fitted power law for the partial cross section.

Table 2. State-selective cross sections for the production of Ar^{2+}(^3P, ^1D, ^1S) ions at electron energies near the ionisation threshold.

E_{el} (eV)	$\sigma(^3P)$ (10^{-19} cm^2)	$\sigma(^1D)$ (10^{-19} cm^2)	$\sigma(^1S)$ (10^{-20} cm^2)
44	0.11	—	—
45	0.78	—	—
46	2.1	0.08	—
47	4.0	0.4	—
48	6.5	1.1	0.07
49	9.7	2.1	0.58
50	13.5	3.5	1.6
51	18.0	5.3	3.1
52	—	7.6	5.1
53	—	10	7.7
54	—	—	11

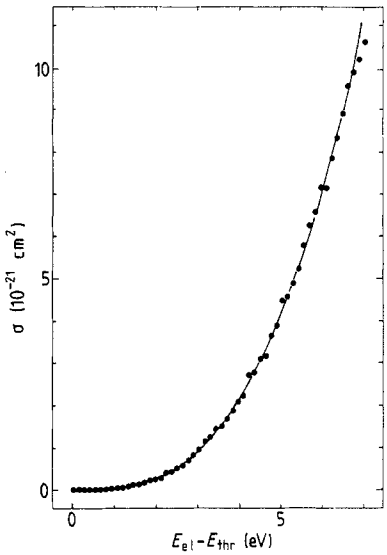

Figure 6. Partial cross section for Ar^{3+} near threshold. The data are fitted to a power law $\sigma \sim (E_{el}-E_{thr})^3$ (full curve).

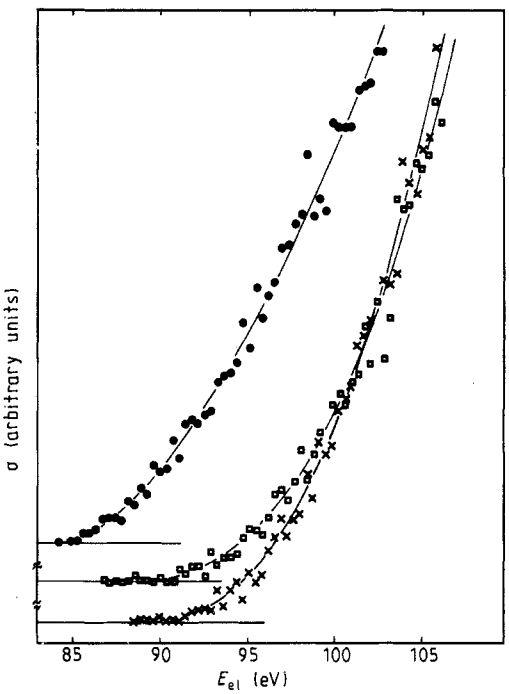

Figure 7. State-selective cross section for the production of Ar in the $^4S^\circ$ ground state (●) and the $^2D^\circ$ (□) and $^2P^\circ$ (×) metastable states. Full curves are fitted power functions.

ions again are formed in different electronic states which can be separated by the help of a single-electron-capture reaction in argon (Binder *et al* 1987). The energy spectra of doubly charged ions yield information on the electronic state of the primary Ar^{3+} ion. After correcting the data with the extraction efficiency the relative cross sections were obtained. The results are shown in figure 7. The corresponding κ values are 1.7, 2.7 and 2.5 for the ground state $^4S^o$ and the metastable $^2D^o$ and $^2P^o$ states respectively, i.e. the exponent is significantly lower for the cross section of the quartet state.

In the case of Ar^{4+}, state-selective measurements have not been successful until now, because the intensities of the secondary-ion signal have been too small. The partial ionisation cross section near threshold (figure 8) scales like $\sigma \sim (E_{el} - E_{thr})^{5/2}$, whereas from the phase space consideration an exponent of the order of 4 is expected. As the partial curve is added up from different states, the exponents for the state-selective cross sections may be even smaller than 2.5. In order to prove this discrepancy and show the sensitivity of the applied fit we have plotted the fourth root of the cross section against the electron impact energy and have also shown $\sigma^{2/5}$ for comparison (figure 9). A straight line is obtained for $\kappa = 2.5$ only and an extrapolation of the fourth root plot to zero will lead to an ionisation threshold which differs by about 10 eV from the values given in the literature (see e.g. Bashkin and Stoner 1978). This difference is much too large to be explained by experimental errors. Therefore we believe that an exponent of 4 can be excluded by the measurements.

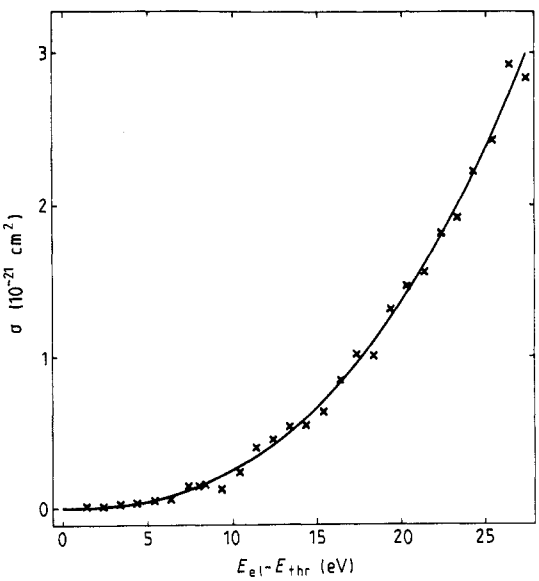

Figure 8. Partial cross section for the production of Ar^{4+} (obtained from the reaction $e^- + Ar \rightarrow 5e^- + Ar^{4+}$). The experimental data can be represented by a power law $\sigma \sim (E_{el} - E_{thr})^{5/2}$ (full curve).

An overview of the present results is given in table 3 and in figure 10, where the fractional exponents κ/q are plotted against the charge state q resulting from single-electron impact near the ionisation threshold. Whereas for $q = 2$ and partly for $q = 3$ our experimental results may still be regarded to be in agreement with the above mentioned q scaling, our results clearly show a decreasing behaviour of κ/q with

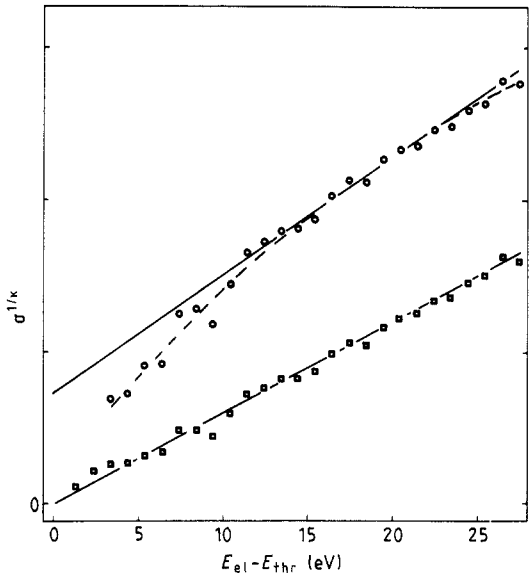

Figure 9. $\sigma^{1/\kappa}$ plot of the Ar^{4+} cross section (obtained from the reaction $e^- + Ar \rightarrow 5e^- + Ar^{4+}$) near threshold. ○, $\kappa = 4$; □, $\kappa = 2.5$.

Table 3. Fit parameters. Near-threshold cross sections have been fitted by using the threshold law $\sigma_i = \sigma_0^{(i)}(E_{el} - E_{thr})^{\kappa i}$, where the index i corresponds either to the partial cross sections for producing Ar^{2+}, Ar^{3+} or Ar^{4+} or to the state-selective cross section describing the production of $Ar^{2+}(^3P, ^1D, ^1S)$ of $Ar^{3+}(^4S^o, ^2D^o, ^2P^o)$.

Final charge state	Electronic state	E_{thr} (eV)	κ	σ_0 ($cm^2\,eV^{-\kappa}$)
2	Sum	43.39	2.6	1.3×10^{-20}
2	^3P	43.39	2.0	2.8×10^{-20}
2	^1D	45.13	2.3	9.6×10^{-21}
2	^1S	47.51	2.0	2.5×10^{-21}
3	Sum	84.13	3.0	3.3×10^{-23}
3	$^4S^o$	84.13	1.7	3.6×10^{-22}
3	$^2D^o$	86.74	2.7	1.8×10^{-23}
3	$^2P^o$	88.45	2.5	1.5×10^{-23}
4	Sum	143.94	2.5	9.7×10^{-25}

increasing q, yielding a κ/q value for $q = 4$ which is definitely much smaller than one. This finding will be the subject of further experimental investigations.

4. Conclusion

We have described experimental results on the multiple ionisation of neutral Ar atoms by single-electron impact. Partial as well as (in some cases) state-selective ionisation cross sections for the production of Ar^{3+}, Ar^{4+}, Ar^{5+} and Ar^{6+} are reported for electron energies from threshold to about 800 eV. Where energetically possible, inner-shell processes turned out to be very effective in producing multiply charged ions via Auger

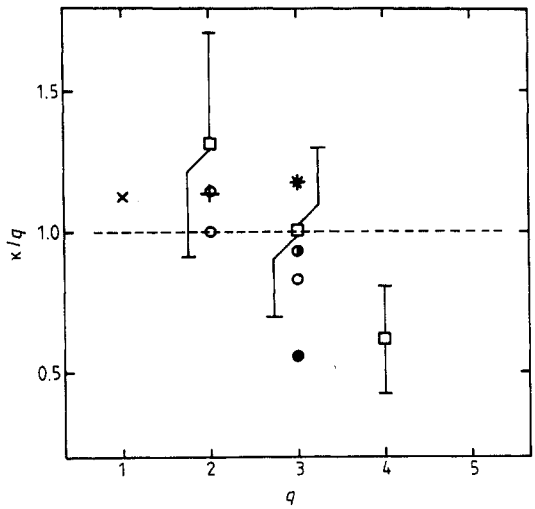

Figure 10. Fractional exponents κ/q for q-fold ionisation: - - -, Wannier (1955); ×, Wannier (1953); +, Klar and Schlecht (1977); *, Grujic (1983); □, present results, partial cross sections; ○, present results, state-selective cross sections for $Ar^{2+}(^3P, ^1D, ^1S)$; ●, ◑, ○, present results, state-selective cross sections for $Ar^{3+}(^4S^o, ^2D^o, ^2P^o$ respectively).

cascades and shake-off mechanisms. Near the ionisation threshold, cross sections can be scaled by a power law $(E_{el} - E_{thr})^{\kappa}$, where the exponent κ is found to be smaller than q for higher charge states.

Acknowledgments

This work has been performed under the auspices of a grant from the Deutsche Forschungsgemeinschaft Bonn-Bad Godesberg which is gratefully acknowledged.

References

Bashkin S and Stoner J O Jr 1978 *Atomic Energy-level and Grotrian Diagrams* vol 2 (Amsterdam: North-Holland)
Binder J, Huber B A, Koslowski H R and Wiesemann K 1987 *J. Phys. B: At. Mol. Phys.* **20** 2713-21
Brion C E and Thomas G E 1968 *Int. J. Mass Spectrom. Ion. Phys.* **1** 25-39
Carlson T A, Hunt W E and Krause M O 1966 *Phys. Rev.* **151** 41-7
Gaudin A and Hageman R 1967 *J. Chim. Phys.* **64** 1209-21
Grujic P 1983 *Phys. Lett.* **96A** 233-5
—— 1986 *Comment. At. Mol. Phys.* **18** 47-74
Huber B A and Kahlert H-J 1983 *J. Phys. B: At. Mol. Phys.* **16** 4655-69
Kahlert H-J, Huber B A and Wiesemann K 1983 *J. Phys. B: At. Mol. Phys.* **16** 449-59
Kahlert H-J, Wiesemann K and Huber B A 1985 *Ann. Phys., Lpz.* **42** 133-41
Kiefer L J and Dunn G H 1966 *Rev. Mod. Phys.* **38** 1-35
Klar H and Schlecht W 1976 *J. Phys. B: At. Mol. Phys.* **9** 1699-711
Lotz 1967 *Z. Phys.* **206** 205-11
Märk T D and Dunn G H (ed) 1985 *Electron Impact Ionization* (Berlin: Springer)
Müller A and Frodl R 1980 *Phys. Rev. Lett.* **44** 29
Rau A R P 1984a *Electronic and Atomic Collisions* ed J Eichler *et al* (Amsterdam: Elsevier) p 711
—— 1984b *Phys. Rep.* **110** 369-87

Read F H 1985 *Electron Impact Ionisation* ed T D Märk and G H Dunn (Berlin: Springer) pp 42–88
Schram B L, Boerboom H J H and Kistemaker J 1966 *Physica* **32** 197–208
Sevier K D 1979 *At. Data Nucl. Data Tables* **24** 341–71
Tawara H, Kato T and Ohnishi M 1985 *Report IPPJ-AM-37* Institute of Plasmaphysics, Nagoya
Wannier G H 1953 *Phys. Rev.* **90** 817–25
—— 1955 *Phys. Rev.* **100** 1180
Wiesemann K, Puerta J and Huber B A 1987 *J. Phys. B: At. Mol. Phys.* **20** 587–603